

AD-A179 648

MEASUREMENT OF SEPARATE VELOCITY PRESSURE AND  
TEMPERATURE COMPONENTS IN T. (U) PRINCETON UNIV NJ DEPT  
OF MECHANICAL AND AEROSPACE ENGINEERIN..

1/1

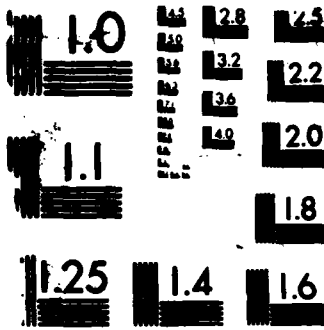
UNCLASSIFIED

R NILES ET AL. JUN 85 NAE-1707

F/G 28/4

NL





MICROCOPY RESOLUTION TEST CHART  
NATIONAL BUREAU OF STANDARDS-1963-A

AD-A179 648

AFOSR-TD- 87-0891

2

Princeton University

DTIC FILE COPY

MEASUREMENT OF SEPARATE VELOCITY, PRESSURE,  
AND TEMPERATURE COMPONENTS IN TURBULENT  
NITROGEN SUPERSONIC FLOWS

By

R. Miles, A. Smits, and M. Zimmermann

FINAL TECHNICAL REPORT

For the Period  
5/15/83 - 8/14/84

U.S. Air Force Office of Scientific Research  
Research Contract #AFOSR-83-0224



This document has been approved  
for public release and sale; its  
distribution is unlimited.

Department of  
Mechanical and  
Aerospace Engineering

DTIC  
ELECTE  
APR 27 1987  
S D  
E

87 4 23 074

2

**AIR FORCE OFFICE OF SCIENTIFIC RESEARCH (AFSC)**  
**NOTICE OF TRANSMITTAL TO DTIC**  
This technical report has been reviewed and is  
approved for public release IAW AFR 190-12.  
Distribution is unlimited.  
**MATTHEW J. KERPER**  
Chief, Technical Information Division

**MEASUREMENT OF SEPARATE VELOCITY, PRESSURE,  
AND TEMPERATURE COMPONENTS IN TURBULENT  
NITROGEN SUPERSONIC FLOWS**

By

R. Miles, A. Smits, and M. Zimmermann

**FINAL TECHNICAL REPORT**

For the Period  
5/15/83 - 8/14/84

U.S. Air Force Office of Scientific Research  
Research Contract #AFOSR-83-0224

Approved for public release;  
distribution unlimited.

Physics Materials Laboratory  
Mechanical & Aerospace Engineering Department

PRINCETON UNIVERSITY  
Princeton, NJ 08544

MAE-1707

June 1985

**DTIC**  
**ELECTE**  
APR 27 1987  
**S** **D**  
**E**

Unclassified

SECURITY CLASSIFICATION OF THIS PAGE (When Data Entered)

REPORT DOCUMENTATION PAGE		READ INSTRUCTIONS BEFORE COMPLETING FORM
1. REPORT NUMBER <b>AFOSR-TR- 87-0891</b>	2. GOVT ACCESSION NO.	3. RECIPIENT'S CATALOG NUMBER
4. TITLE (and Subtitle) MEASUREMENT OF SEPARATE VELOCITY, PRESSURE, AND TEMPERATURE COMPONENTS IN TURBULENT NITROGEN SUPERSONIC FLOWS	5. TYPE OF REPORT & PERIOD COVERED Final Technical 5/15/83 - 8/14/84	
	6. PERFORMING ORG. REPORT NUMBER MAE-1707	
7. AUTHOR(s) R. Miles, A. Smits, and M. Zimmermann	8. CONTRACT OR GRANT NUMBER(s) AFOSR-83-0224	
9. PERFORMING ORGANIZATION NAME AND ADDRESS Mechanical & Aerospace Engineering Dept. Princeton University, Physics Materials Lab Princeton, NJ 08544	10. PROGRAM ELEMENT, PROJECT, TASK AREA & WORK UNIT NUMBERS 61102F/2307/A2	
11. CONTROLLING OFFICE NAME AND ADDRESS United States Air Force Air Force Office of Scientific Research Bldg 410, BAFB D.C. 20332 NA	12. REPORT DATE June 1985	
	13. NUMBER OF PAGES 24	
14. MONITORING AGENCY NAME & ADDRESS (if different from Controlling Office) Same as 11	15. SECURITY CLASS. (of this report) Unclassified	
	15a. DECLASSIFICATION/DOWNGRADING SCHEDULE	
16. DISTRIBUTION STATEMENT (of this Report)  <b>Approved for public release; distribution unlimited.</b>		
17. DISTRIBUTION STATEMENT (of the abstract entered in Block 20, if different from Report)		
18. SUPPLEMENTARY NOTES (continued)		
19. KEY WORDS (Continue on reverse side if necessary and identify by block number) Turbulence; Resonant Doppler Velocimeter; Laser Induced Fluorescence; Computer Simulation; Sodium Seeding; Flow Diagnostics;		
20. ABSTRACT (Continue on reverse side if necessary and identify by block number) → A computer model is used to simulate the measurement of fluctuating flow properties using resonant Doppler velocimetry. A narrow linewidth laser excites fluorescence from sodium atoms which are seeded into a nitrogen flow. The sensitivity of the fluorescence to fluctuating flow parameters as a function of laser wavelength is different for each flow parameter. Thus, a scan of the laser wavelength allows separate measurement of the time averaged fluctuations of velocity, temperature, and pressure. →		

(cont)

Computer fits to simulated fluorescence profiles from flows with randomly generated fluctuating parameters are shown to accurately reproduce the mean and standard deviations of each separate parameter. Cross correlations are also extracted, but with less accuracy due largely to truncation error in the computer fitting routine.

Keywords:

( )

1960-1961  
1962-1963

TABLE OF CONTENTS

Page No.

1. INTRODUCTION . . . . . 1

2. ANALYSIS OF THE ABSORPTION-EMISSION PROFILE . . . . . 3

3. SIMULATED DATA GENERATION AND FITTING ROUTINES . . . . . 9

4. ROBUSTNESS OF THE FITTING ROUTINE . . . . . 19

5. CONCLUSION . . . . . 21

6. PERSONNEL ASSOCIATED WITH THE PROJECT . . . . . 22

7. PUBLICATIONS AND REPORTS . . . . . 23

REFERENCES . . . . . 24

<b>Accession For</b>	
NTIS GRA&I	<input checked="" type="checkbox"/>
DTIC TAB	<input type="checkbox"/>
Unannounced	<input type="checkbox"/>
Justification	
By _____	
Distribution/	
Availability Codes	
Dist	Avail and/or Special
A-1	



## 1. INTRODUCTION

This report covers work done during the past year on a pilot study to determine the feasibility of simultaneously measuring temperature, velocity, and pressure fluctuations in a turbulent flow with an optical system based on the Resonant Doppler Velocimeter [1]. The model system studied was sodium seeded into a supersonic nitrogen flow. The methodology may be extended to iodine in nitrogen or air and other atomic and molecular fluorescing species. In the experiment, a laser beam passes through the sample point (or sample plane). As the laser is tuned through the sodium absorption profile, the average and fluctuating components of the fluorescence from the sample point are detected. The purpose of this study is to assess whether the average fluctuating magnitude of all the flow parameters can be separately determined from these measurements.

The procedure we are following consists of four distinct computational steps. The first step is a program which generates artificial data. With the aid of a random number generator this program gives the sampled fluorescence intensities at a variety of separate laser frequencies across the absorption spectrum of the sodium. The second step is a fitting program which uses a nonlinear least squares fitting routine to generate the absorption-emission profile which most closely approximates the average intensity measured at each frequency. The fitted parameters of this profile can be compared to the temperature, pressure, and velocity initially given to the data generation routine to see how accurately this fit reproduces the average static conditions. The third step is a program which generates a temperature, pressure, and velocity sensitivity from the fitted profile. Finally, in the fourth step, these sensitivities



are fitted to the variance of the measured intensities at each laser frequency in order to yield the turbulent flow parameters.

Although many factors contribute, one can think of the variation of the absorption profile in frequency as being an indication of the velocity fluctuations, the variation in the amplitude as being an indication of the magnitude of the temperature fluctuation, and the variation of the linewidth as being an indication of the pressure fluctuation. For this study we have assumed that the ratio of sodium to nitrogen molecules stays constant, independent of the flow conditions. This will be true so long as the seeding is uniform.

## 2. ANALYSIS OF THE ABSORPTION-EMISSION PROFILE

The sodium transition of interest actually consists of six separate transitions due to the hyperfine splitting of the sodium atom. In this discussion we idealize sodium by considering only one of these transitions. No generality is lost however, and the proper lineshape is later constructed by a weighted sum of six idealized transitions. Saturation and optical pumping have been ignored for the purposes of clarity.

The fluorescence power intensity detected from a unit volume,  $P_{\text{DET}}$ , can be related to the laser power absorbed per unit volume,  $P_{\text{ABS}}$ , as shown in expression (1):

$$P_{\text{DET}} = P_{\text{ABS}} \times \frac{\text{optical relaxation rate}}{\text{quenching rate} + \text{optical relaxation rate}} \times \text{collection efficiency} \quad (1)$$

If optical relaxation is much stronger than quenching then all of the power that goes in is reradiated and the power measured is the absorbed power reduced by the collection efficiency of the detection apparatus. This collection efficiency includes the collection aperture of the optics, the optical filter transmission, and the efficiency of the photodetector. A collection efficiency better than a few percent is difficult to achieve.

If sodium is seeded into nitrogen, the quenching rate predominates over the optical relaxation rate and the detected signal is significantly reduced. This means that some of the energy is lost via non-radiative channels to the nitrogen. The optical relaxation rate is the number of photons emitted per second and equals the natural lifetime of the sodium in the excited state:

$$\text{OPTICAL RELAXATION RATE} = \frac{1}{\tau_{\text{Na}}} = 6.25 \times 10^7 \text{ sec}^{-1} \quad (2)$$

This rate is independent of collisions. The quenching rate is determined by the number of collisions per second between sodium atoms and nitrogen molecules. As shown in expression (3) this can be written as the nitrogen density,  $N_{N_2}$ , times the relative velocity between the sodium and nitrogen,  $v_{rel}$ , times a quenching collision cross section,  $Q$ .

$$\text{QUENCHING RATE} = N_{N_2} v_{rel} Q \quad (3)$$

For the purposes of our calculation we are interested in the variation of the detected power with respect to velocity, temperature, and pressure. The relative velocity between the sodium and nitrogen is related to the temperature since the sodium and nitrogen are considered well-mixed and thus moving with the same average velocities. This relation is shown in expression (4) where  $k$  is Boltzmann's constant,  $T$  is the temperature, and  $\mu$  is the reduced mass of the nitrogen and the sodium.

$$v_{rel} = \sqrt{\frac{8kT}{\pi\mu}} \quad (4)$$

The quenching cross section is also related to the temperature, however, its exact temperature dependence in the range of temperatures and pressures in which we expect to operate is not well-determined. From reference [2] we approximate this cross section as

$$Q \approx 10^{-16}/T \quad (\text{m}^2) \quad (5)$$

Combining the above relationships we then arrive at an expression for the variation of the detected power which can be written:

$$P_{DET} = \frac{K\sqrt{T}}{N_{N_2}} P_{ABS} \quad (6)$$

where  $K$  is a constant and a large quenching rate has been assumed.

The total absorbed power over a small pathlength  $\Delta x$  is given in the following expression:

$$P_{\text{ABS}} = I_L \left\{ 1 - \exp(-\Gamma(\nu)\Delta x) \right\} A \quad (7)$$

where  $I_L$  is the incident laser intensity (watts/m<sup>2</sup>) measured at  $\Delta x=0$ ,  $A$  is the beam area, and  $\Gamma(\nu)$  is the absorption constant which will be discussed shortly. Assuming that the amount of light absorbed over the distance  $\Delta x$  is small, the exponent can be expanded and the volume divided out to give the expression for the absorbed power per unit volume for the case of low optical density

$$P_{\text{ABS}} = I_L \Gamma(\nu) \quad (8)$$

The absorption constant,  $\Gamma(\nu)$ , involves a line strength factor, the sodium density, and a lineshape function

$$\Gamma(\nu) = (\pi r_o c f) (N_{\text{Na}}) (V(\nu)) \quad (9)$$

The line strength factor includes  $r_o = 2.82 \times 10^{-15}$  m,  $c$  = the speed of light, and  $f$ , which is the oscillator strength and varies between .3 and .6 for the transitions in which we are interested. These factors are not affected by temperature, pressure, or velocity, and can thus be combined together as a single constant. The lineshape factor  $V(\nu)$  is due to a combination of thermal broadening and collision broadening. An excellent approximation for this is the Voigt profile in which the normalized thermal broadening factor is convolved with a normalized collision broadening factor. Experiments have shown that this profile fits the data to high accuracy. The thermal broadening factor is written

$$g(\nu) = \sqrt{\frac{\lambda n^2}{\pi}} \frac{1}{\Delta \nu_T} \exp\left[-\lambda n^2 \left(\frac{\nu - \nu_0}{\Delta \nu_T}\right)^2\right] \quad (10)$$

where

$$\nu_0 = 5.1 \times 10^{14} \left(1 + \frac{\bar{V}}{c} \cos\theta\right) \quad (11)$$

is the frequency of the absorption line center of sodium shifted by the average velocity component in the direction of the laser illumination, and  $\Delta\nu_T$  is the thermal linewidth

$$\Delta\nu_T = \nu_0 \sqrt{\frac{8 \ln 2}{m_{\text{Na}}} \frac{kT}{c^2}} = 7.57 \times 10^7 \sqrt{T} \quad (\text{Hz}) \quad (12)$$

This thermal broadening factor occurs due to the Doppler shift of the sodium atoms as seen by the incident radiation as they move about with random thermal fluctuations. This expression is normalized so that when integrated over all frequencies one finds

$$\int g(\nu) d\nu = 1 \quad (13)$$

The collision broadening factor is written

$$g(\nu) = \frac{1}{\pi} \frac{\Delta\nu_L/2}{(\nu - \nu_0)^2 + (\frac{\Delta\nu_L}{2})^2} \quad (14)$$

where again  $\nu_0$  is the center frequency for absorption shifted by the average velocity component, and  $\Delta\nu_L$  is the collision linewidth

$$\Delta\nu_L = \frac{1}{2\pi} \sqrt{2 N_{\text{N}_2} v_{\text{rel}} \sigma_b} \quad (15)$$

In this expression  $\sigma_b$  is the collision broadening cross section which, again, is not well known at the low temperatures where our measurements are to be taken. An approximation from reference [3] gives

$$\sigma_b \approx 1.28 \times 10^{-18} T^{-0.2} \quad (\text{m}^2) \quad (16)$$

Note that the thermal broadening depends only on temperature while the collision broadening depends on both temperature and pressure. If we rewrite the collision broadening factor in terms of pressure and temperature we find

$$\Delta\nu_L = 1.21 \times 10^6 P T^{-.7} \quad (\text{Hz}) \quad (17)$$

where pressure is in Pascals and temperature in Kelvin. The collision broadening arises from the fact that each time a sodium atom undergoes a collision with a nitrogen molecule, the atom is perturbed. As expected from the uncertainty principle, the energy levels of the atom become broadened because the atom exists in a pure state for a shorter period of time. Since the atom's energy is related to the absorption frequency, that leads to a broadening of the spectrum.

The Voigt profile arises due to the fact that both broadening mechanisms simultaneously occur. Thus, each "velocity group" under the thermal curve is separately collision broadened. The overall curve shape, then, becomes equivalently a weighted sum of collision broadened subgroups. This is written

$$V(\nu) = \int_{-\infty}^{\infty} \ell(\nu - \Delta) g(\Delta) d\Delta \quad (18)$$

where  $\Delta$  is a dummy variable of integration.

From equations (6), (8) and (9) we find our final expression for the detected power per unit volume.

$$P_{\text{DET}} = I_L K \frac{N_{\text{Na}}}{N_{\text{N}_2}} \sqrt{T} V(\nu) = f(T, P, V, \nu) \quad (19)$$

Assuming a constant laser intensity, the detected power is only a function of temperature, pressure, velocity, and the laser frequency,  $\nu$ . The ratio of the density of sodium to the density of nitrogen is constant assuming uniform seeding.

In general, the laser will be tuned in discrete steps across the absorption spectrum of the sodium. At each laser frequency, the detected power intensity and its fluctuations will be measured. If desired, the fluctuations can be resolved into separate spectral components. For this discussion, however, we will assume that some number of samples are taken at each laser frequency. In the absence of fluctuations of the temperature, pressure, or velocity, each of these samples yields the same measured power. If fluctuations are present, the measured power intensity will vary and the magnitude of that variation will depend upon the sensitivity of the absorption-emission curve to that particular parameter.

### 3. SIMULATED DATA GENERATION AND FITTING ROUTINES

In order to generate simulated data for the fitting routines, average values of temperature, pressure, and velocity are first selected. Following that, a desired maximum fluctuation limit for each of these parameters is chosen. The program multiplies this fluctuation limit by a random number between  $-0.5$  and  $+0.5$  and adds that to the appropriate average parameter. This is done for each simulated sample. Thus, if 51 separate laser frequencies are chosen and 25 samples taken at each frequency, 1275 values of temperature, pressure, and velocity are separately generated. The program then calculates the average and standard deviation of temperature, pressure, and velocity. It is these values which the fitting routines are expected to reproduce. At each laser frequency, the program also calculates the detected intensity for each sample taken at that frequency using the randomly varying temperature, pressure, and velocity.

Figures 1 through 5 are examples from the data generation program and also serve to demonstrate the unique signature of each varying parameter. The static conditions were chosen to be those of the Mach 3.4 nitrogen flow in which we first undertook these measurements [4]. These were  $T = 100^\circ\text{K}$ , and  $P = 1700$  Pa. The average velocity in the illumination direction is assumed to be 0 (a nonzero average velocity component will simply shift the spectrum in wavelength). Figure 1 shows the result for no variations in flow parameters. The intensity scale is arbitrary and the wavelength scale is just the number of wavelength steps taken. In Figure 2 a maximum fluctuation of  $\pm 25\%$  or  $\pm 25^\circ\text{K}$  in the temperature is simulated with pressure and velocity held constant. At each wavelength, 25 samples are taken. In Figure 3 a maximum fluctuation of  $\pm 25\%$  or  $\pm 425$  Pa in the pressure is simulated with



Figure 1. Absorption-emission profile at  $T = 100^\circ\text{K}$ ,  $P = 1700\text{ Pa}$ ,  $v = 0\text{ m/sec}$ .

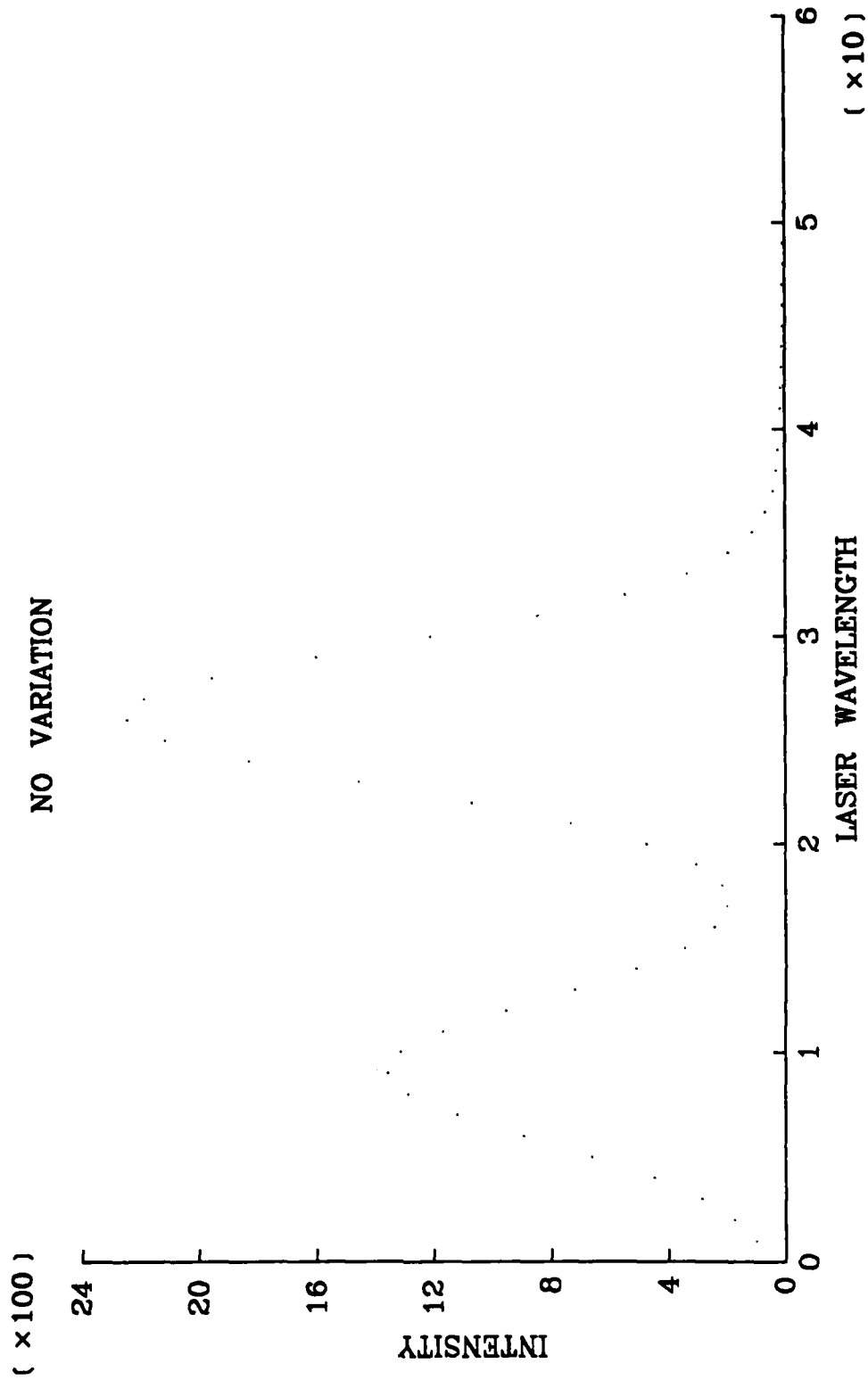


Figure 2 Absorption-emission profile with  $T = 100 \pm \leq 25^\circ\text{K}$ ,  $P = 1700 \text{ Pa}$ ,  $v = 0. \text{m/sec}$ .

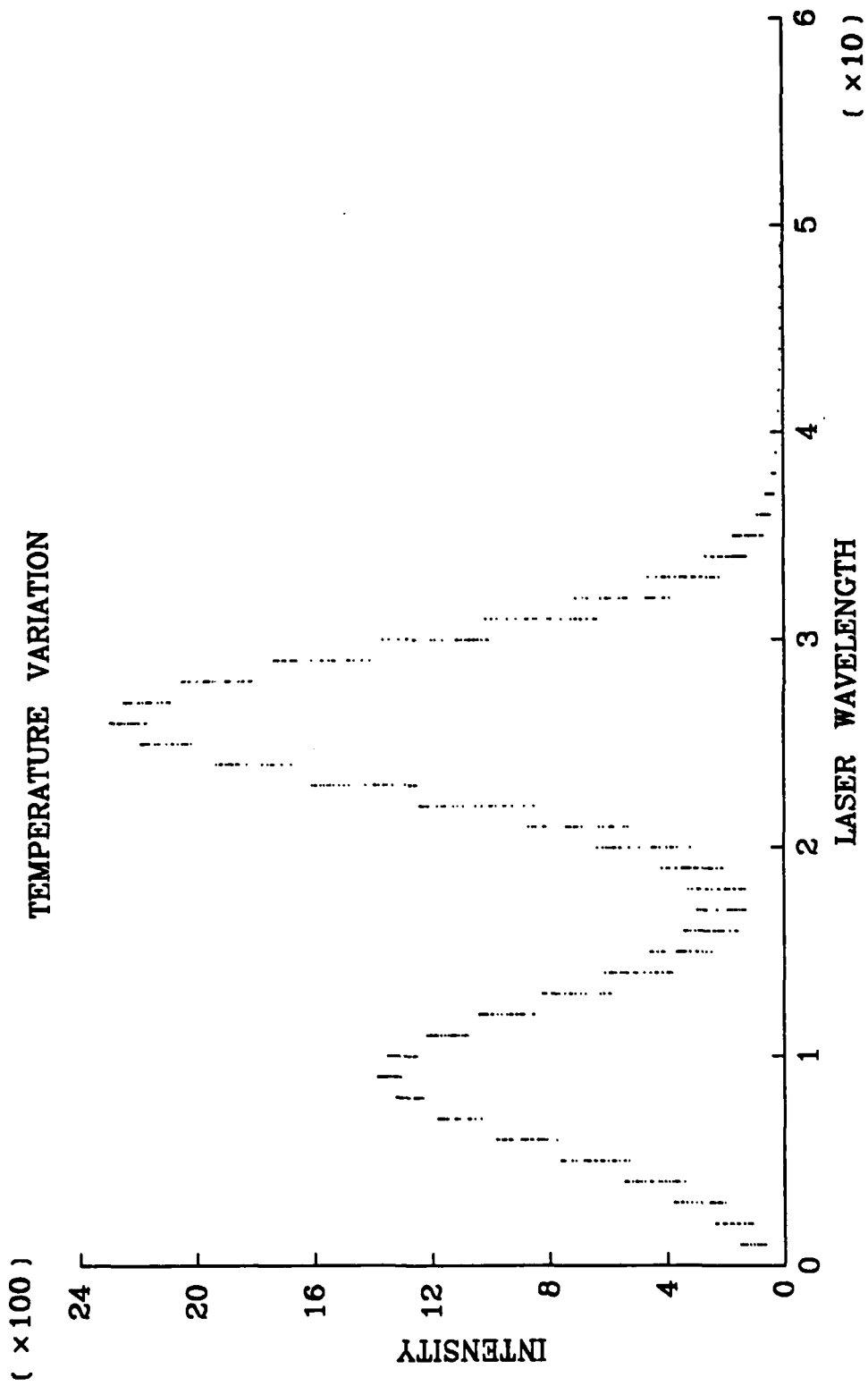
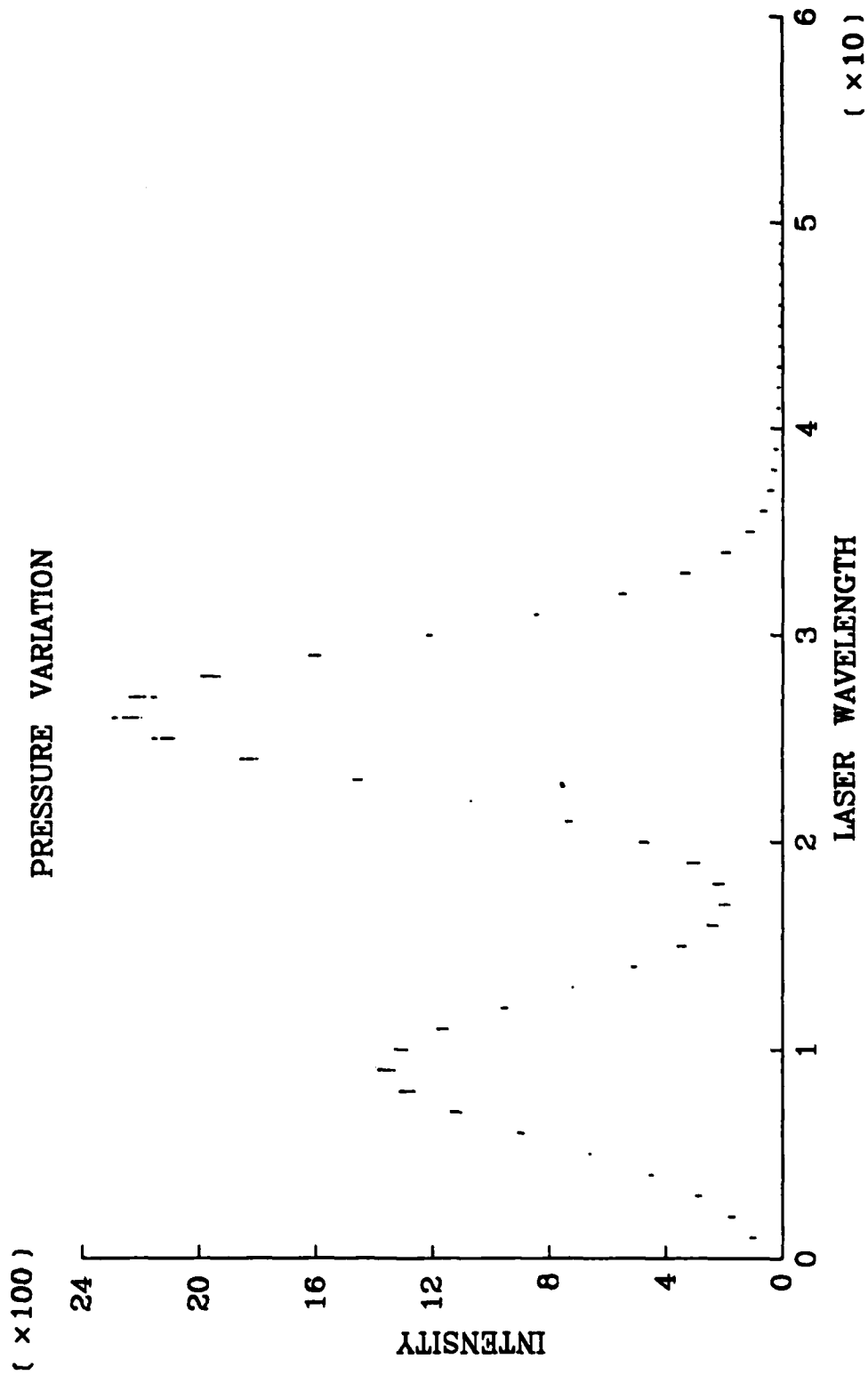


Figure 3. Absorption-emission profile with  $T = 100^\circ\text{K}$ ,  $P = 1700 \pm \leq 425 \text{ Pa}$ ,  $v = 0 \text{ m/sec}$ .



temperature and velocity constant. Similarly Figure 4 is a  $\pm 25$  m/sec variation in the velocity component in the illuminating laser direction with temperature and pressure constant. Figure 5 shows the curve with all the parameters simultaneously varying  $\pm 25\%$ .

The rather large variations were chosen to make the characteristics of these variations apparent. Note, particularly, that the velocity variations do not affect the measurement at the maxima and minimum of the curve. The pressure variations do not affect the curve near the half power points. The temperature variations are seen throughout. Thus it should be possible to separately determine the contribution of each from the character of the measured curve.

At each laser wavelength, the data generation program also calculates the average measured intensity and the variance of the intensity. The average intensities are passed to a curve fitting routine which produces a fit yielding the average temperature, pressure, and velocity. This step is important since the sensitivities of the detected intensity to variations in temperature, pressure and velocity, depend strongly on the average temperature, pressure, and velocity about which these variations take place. For example, if the pressure is very low, the collision broadening factor becomes negligible and the Voigt lineshape reduces to the thermal broadening. As a consequence, the detected intensity becomes insensitive to pressure variations. The exact form of the sensitivity must be calculated in order to perform the fit to determine turbulence parameters. The fitting procedure uses the ZXSSQ routine from the IMSL Fortran library. This is a standard fitting routine which proceeds by trial and error. Given the fact that the characteristics of the Voigt profile are well understood, other fitting routines could conceivably be devised to provide more rapid convergence. The fit of the average

Figure 4. Absorption-emission profile with  $T = 100^\circ\text{K}$ ,  $P = 1700 \text{ Pa}$ ,  $v = \pm \leq 25 \text{ m/sec}$ .

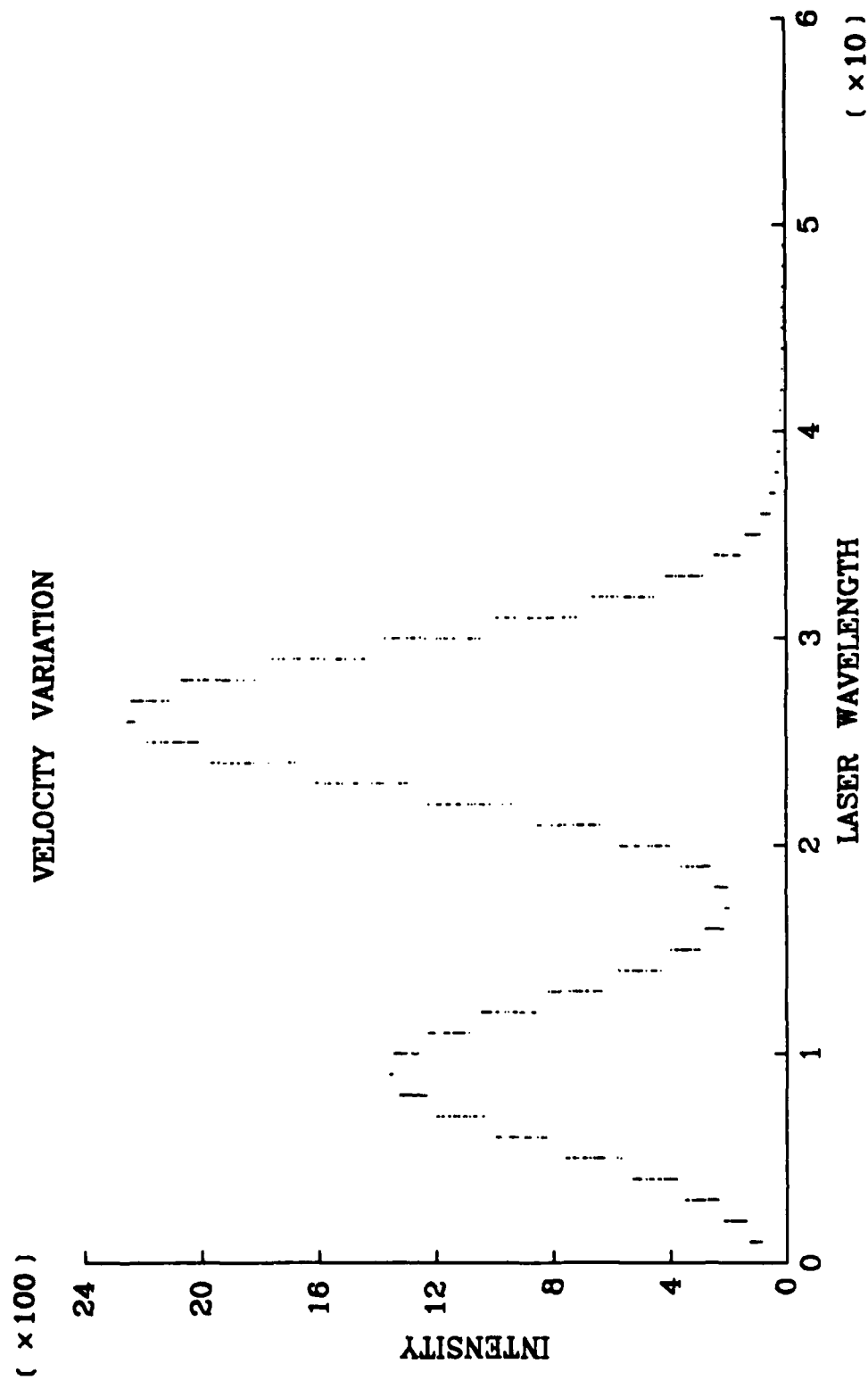
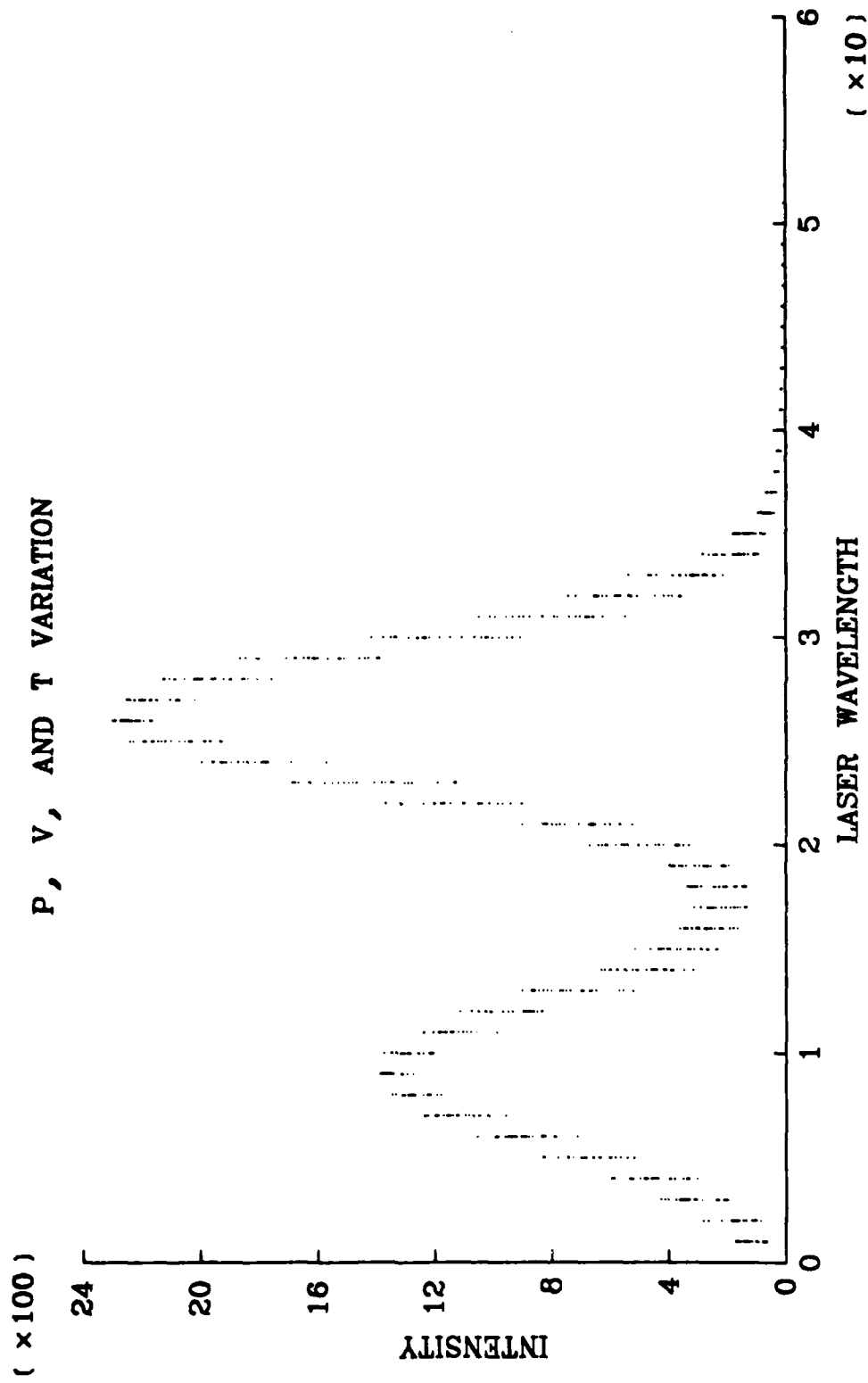


Figure 5. Absorption-emission profile with  $T = 100 \pm \leq 25^\circ\text{K}$ ,  $P = 1700 \pm \leq 425 \text{ Pa}$ ,  $v = \pm \leq 25 \text{ m/sec}$ .



detected intensities should reproduce with reasonable accuracy the average temperature, pressure, and velocity, generated by the data simulation routine.

Once the fitted values of temperature, pressure and velocity have been found, the sensitivities at each frequency are calculated. These sensitivities are essentially the derivatives of the detected power with respect to each parameter. In the small signal approximation, we can write the detected power in a Taylor expansion:

$$P_{\text{DET}}(n, \nu) = \bar{P}_{\text{DET}}(\nu) + \left(\frac{\partial P_{\text{DET}}(\nu)}{\partial \nu}\right)_{T, P} \Delta \nu(n) + \left(\frac{\partial P_{\text{DET}}(\nu)}{\partial T}\right)_{\nu, P} \Delta T(n) + \left(\frac{\partial P_{\text{DET}}(\nu)}{\partial P}\right)_{T, \nu} \Delta P(n) \quad (20)$$

where  $n$  indicates the  $n$ th sample at laser frequency  $\nu$ . The variance of the detected intensity at any laser frequency  $\nu$ , is then

$$\overline{(\delta P_{\text{DET}}(\nu))^2} = \frac{1}{n} \sum_n \left\{ S_{\nu}(\nu) \Delta \nu + S_T(\nu) \Delta T + S_P(\nu) \Delta P \right\}^2 \quad (21)$$

where the sensitivities are defined

$$S_{\nu}(\nu) = \frac{\partial P_{\text{DET}}(\nu)}{\partial \nu} \quad (22)$$

$$S_T(\nu) = \frac{\partial P_{\text{DET}}(\nu)}{\partial T} \quad (23)$$

$$S_P(\nu) = \frac{\partial P_{\text{DET}}(\nu)}{\partial P} \quad (24)$$

This then yields:

$$\begin{aligned} \overline{\delta P_{\text{DET}}(\nu)^2} &= S_{\nu}^2(\nu) \overline{\Delta \nu^2} + S_T^2(\nu) \overline{\Delta T^2} + S_P^2(\nu) \overline{\Delta P^2} + 2S_{\nu}(\nu)S_P(\nu) \overline{\Delta \nu \Delta P} \\ &+ 2S_{\nu}(\nu)S_T(\nu) \overline{\Delta \nu \Delta T} + 2S_P(\nu)S_T(\nu) \overline{\Delta P \Delta T} \end{aligned} \quad (25)$$

If the fluctuations are correlated, the products  $\Delta v \Delta P$ ,  $\Delta v \Delta T$ , and  $\Delta P \Delta T$  give the correlation constants. Thus, in general, a six parameter fit will yield the mean square variation of velocity, temperature, and pressure, plus the three correlation constants. Of course, the fit must be performed over numerous laser frequencies and the sensitivities must be non-degenerate in order to provide viable results.

Table 1 shows a sample output from the data generation routine as well as the curve-fitting and the six parameter fitting routines. In this example, variations of  $\pm 2.5\%$  in temperature and pressure and  $\pm 2.5$  m/sec in velocity have been used. Note that the curve-fitting routine reproduces the values of  $\bar{T}$ ,  $\bar{v}$ , and  $\bar{P}$  rather well. The six parameter fit reproduces the standard deviation of T, P, and v with reasonable accuracy. The correlation constants should all be zero. The value of .52 for the v-P correlation is a spurious result arising from truncation error in the computer routine. We are currently reworking the routine to minimize this problem.



Table 1. Input and fitted results for a maximum simultaneous variation of  $\pm 2.5\%$  for T and P and  $\pm 2.5$  m/sec for v.

---

Input Parameters were:

T = 100.00 Kelvin  
 P = 1700.00 Pascal  
 v = 0.0 meters/sec  
 $\Delta T$  = 5.00  
 $\Delta P$  = 85.00  
 $\Delta v$  = 5.00  
 Step = 100000000. Hertz  
 Number of Steps = 51  
 Samples per Step = 25

---

Output of Data Simulation Routine:

$\bar{T}$  = 99.97  
 $\bar{P}$  = 1700.45  
 $\bar{v}$  = 0.07  
 $(\overline{\Delta T^2})^{1/2}$  = 1.48  
 $(\overline{\Delta P^2})^{1/2}$  = 24.06  
 $(\overline{\Delta v^2})^{1/2}$  = 1.42

---

Output of the Curve-Fitting Routine:

T-fitted = 100.00  
 P-fitted = 1700.64  
 v-fitted = 0.09

---

Output of the Six Parameter Variation-Fitting Routine:

$(\overline{\Delta T^2})^{1/2}$ -fitted = 1.26  
 $(\overline{\Delta P^2})^{1/2}$ -fitted = 24.09  
 $(\overline{\Delta v^2})^{1/2}$ -fitted = 1.43  
 Correlation of v and P-fitted = 0.52  
 Correlation of v and T-fitted = 0.028  
 Correlation of T and P-fitted = -0.081

---

#### 4. ROBUSTNESS OF THE FITTING ROUTINE

The ability of the fitting routines to properly determine parameter variations is based on the effect those variations will have on the absorption-emission curve. In the high temperature-low pressure regime, the pressure sensitivity is reduced due to the fact that its contribution to the lineshape becomes less important. In order to test our continued ability to observe pressure at high temperatures we ran a three parameter fitting routine (i.e. we neglected the correlations) for 20°K increments between 100°K and 280°K. Pressure was held constant at 1700 Pa. Temperature and pressure were varied  $\pm 5^\circ\text{K}$  and  $\pm 85$  Pa respectively. Velocity was varied a maximum of  $\pm 5$  m/sec. Standard deviations of the actual data were 2.96PK, 48.13 Pa, and 2.84 m/sec. The resultings of the fitting routine are shown in Table 2. Here we see that the fitted values for pressure are reasonably unaffected by temperature. The fitted values for temperature and velocity do appear to have some temperature dependence.

Table 2. Fitting sensitivity to temperature variation.

<u>Input Values</u>			<u>3 Parameter Fitted Values</u>		
Temperature	Pressure	Velocity	$\overline{(\Delta T^2)}^{1/2}$	$\overline{(\Delta P^2)}^{1/2}$	$\overline{(\Delta v^2)}^{1/2}$
100.00	1700.00	0.0	2.47	42.01	2.94
120.00	1700.00	0.0	2.37	49.98	2.94
140.00	1700.00	0.0	2.48	48.51	2.83
160.00	1700.00	0.0	2.50	48.32	2.80
180.00	1700.00	0.0	2.50	48.40	2.78
200.00	1700.00	0.0	2.50	48.46	2.77
220.00	1700.00	0.0	2.50	48.51	2.76
240.00	1700.00	0.0	2.51	48.53	2.75
260.00	1700.00	0.0	2.51	48.56	2.75
280.00	1700.00	0.0	2.52	48.68	2.74

Actual Values:

$$\overline{(\Delta T^2)}^{1/2} = 2.96$$

$$\overline{(\Delta P^2)}^{1/2} = 48.13$$

$$\overline{(\Delta v^2)}^{1/2} = 2.84$$

## 5. CONCLUSION

The results of our work give us strong encouragement that temperature, pressure, velocity, and the three correlation constants can be extracted from the flow measurements. Our computer routine still needs to be upgraded in its precision, but it nonetheless has shown an ability to fit the standard deviation of temperature, pressure, and velocity with reasonable accuracy. Since each value of temperature, pressure, and velocity for each sample is created by an independent random number, we expect no correlation. The fact that, in some cases, significant correlations are calculated indicates that this step of the process must be further explored. We also intend to address the issue of how most efficiently to take data, i.e., many sample points at few laser wavelengths, or vice versa. From Figures 1 through 5, it is important to note that certain wavelengths need to be sampled. For example, the peaks of the curve should be sampled to allow separation of velocity fluctuations from those of temperature and pressure. Similarly, the curves should be sampled near their half-power points to allow separation of the pressure variations from the velocity and temperature. Sampling in the wings of the curve is also important, however, it is in that region that the signal is smallest and, therefore, the vulnerability to noise the greatest.

6. PERSONNEL ASSOCIATED WITH THE PROJECT

Prof. Richard B. Miles                      Principal Investigator

Prof. Alexander J. Smits                    Principal Investigator

Dr. Micha Zimmermann                      Postdoctoral Associate

Jeffrey Berger                               Undergraduate Student

7. PUBLICATIONS AND REPORTS

1. R. Miles, A. Smits, and M. Zimmermann, "Separation of Turbulent Parameters by Laser Induced Fluorescence: A Computer Simulation," American Physical Society, Division of Fluid Dynamics, Providence, RI, November 18-20, 1984, Bulletin of the American Physical Society 29, Paper CK4, New York: American Physical Societ, 1984.
  
2. R. Miles, "Applications of the Resonant Doppler Velocimeter in Flow Visualization and Turbulence," San Francisco, CA, November 26-30, 1984, Technical Digest of the International Conference on Lasers '84, Paper L6, 1984.

REFERENCES

1. S. Cheng, M. Zimmermann, and R. B. Miles, "Supersonic-nitrogen flow-field measurements with the resonant Doppler velocimeter," *Appl. Phys. Lett.* 43, 143 (July 1983).
2. P.L. Lijnse and R. J. Elsenaar, "The Temperature Dependence of the Quenching of Na-D-Doublet by  $N_2$  and  $H_2O$  in Flames of 1500-2500°K," *J. Quant. Spectrosc. Radiat. Transfer* 12, 1115 (1972).
3. M.J. Jongerius, A.R.D. Van Bergen, Tj. Hollander and C. Th. J. Alkemade, "An Experimental Study of the Collisional Broadening of the Na-D Lines by Ar,  $N_2$ , and  $H_2$  Perturbes in Flames and Vapor Cells--I. The Line Core," *J. Quant. Spectrosc. Radiat. Transfer* 25, 1 (1981).
4. S. Cheng, M. Zimmermann, and R.B. Miles, "Separation of time-averaged turbulence components by laser-induced fluorescence," *Phys. Fluids* 26, 874 (April 1983).

END

5-87

DTIC